

# Adsorption of molecular oxygen on doped graphene: atomic, electronic and magnetic properties

Jiayu Dai and Jianmin Yuan\*

*Department of Physics, National University of Defense Technology, Changsha 410073, People's Republic of China*

(Dated: November 24, 2009)

Adsorption of molecular oxygen on B-, N-, Al-, Si-, P-, Cr- and Mn-doped graphene is theoretically studied using density functional theory in order to clarify if O<sub>2</sub> can change the possibility of using doped graphene for gas sensors, electronic and spintronic devices. O<sub>2</sub> is physisorbed on B-, and N-doped graphene with small adsorption energy and long distance from the graphene plane, indicating the oxidation will not happen; chemisorption is observed on Al-, Si-, P-, Cr- and Mn-doped graphene. The local curvature caused by the large bond length of X-C (X represents the dopants) relative to C-C bond plays a very important role in this chemisorption. The chemisorption of O<sub>2</sub> induces dramatic changes of electronic structures and localized spin polarization of doped graphene, and in particular, chemisorption of O<sub>2</sub> on Cr-doped graphene is antiferromagnetic. The analysis of electronic density of states shows the contribution of the hybridization between O and dopants is mainly from the *p* or *d* orbitals. Furthermore, spin density shows that the magnetization locates mainly around the doped atoms, which may be responsible for the Kondo effect. These special properties supply a good choice to control the electronic properties and spin polarization in the field of graphene engineering.

PACS numbers: 61.48.De, 68.43.-h, 75.20.Hr, 73.22.-f

## I. INTRODUCTION

Graphene has been becoming a new star in a lot of fields after its successful fabrication<sup>1-3</sup>, especially for the application of two aspects below because of the many reasons for the renewed interest: first, it is very potential to apply graphene as gas sensors with high sensitivity because the transport properties exhibit large changes upon exposure to several gases such as NO<sub>2</sub><sup>4</sup>. Graphene can be used as an excellent sensor material because of its special properties such as two dimensional property maximizing the interaction of adsorbates on the layer, low Johnson noise<sup>2,5-7</sup>, and few crystal defects<sup>2,5,6</sup>. This tells us the electronic properties of graphene system can be sensitive to the adsorption of gases. Second, there is an extraordinary interest in the electronic band properties and magnetic order in graphene-related materials that can be put into use as the next-generation electronic devices and recording media, magnetic inks, spin qubits and spintronic devices<sup>3,8,9</sup>, which can use the advantages of high mobility of electrons in graphene and long coherence times in carbon-based materials. A few investigations have been performed until now to search for the potential application of graphene or graphene nanoribbons as gas sensors<sup>10,11</sup>. However, it has been shown that intrinsic graphene can only physisorb most of gas molecules<sup>11-13</sup> and has no band gap and spin polarization. This, for example, prevents the use of graphene in making gas sensors, transistors and spintronic devices.

In order to improve the sensitivity for gases and the electronic structures in graphene and carbon nanotubes (CNTs), the method of doping is usually used. B- and N-doped graphene can also improve gas sensing of CO, NO, NO<sub>2</sub> and NH<sub>3</sub><sup>14</sup>; Al-doped graphene can be sensitive to most of common gases in air<sup>15</sup>; H<sub>2</sub>O on Ti-doped graphene<sup>16</sup>, chlorophenols on Si-doped CNTs<sup>17</sup>

are also reported. Meanwhile, the electronic structures and magnetic properties in graphene and graphene nanoribbons can be changed by doping different atoms such as boron<sup>18</sup>, sulfur and phosphorus<sup>19</sup>, transition metal atoms<sup>20-22</sup>, or by defect engineering<sup>23</sup>, functionalized with different atoms, molecules and clusters<sup>24</sup> and so on. Experimentally, several CNTs and graphene-based materials with different dopants such as nitrogen<sup>25</sup>, boron<sup>26</sup>, phosphorus<sup>27</sup> were also synthesized. It has been shown by these studies that the doped graphene or CNTs materials are very potential for gas sensors, electronics and spintronics.

However, in order to use these materials in reality, the effect of O<sub>2</sub> should be considered, since O<sub>2</sub> is one of the most important gases taking up more than 20% in air. Meanwhile, it has been shown that O<sub>2</sub> can hole-dope semiconductors<sup>28</sup>. Also, gas molecules can change the electronic and magnetic properties of graphene and graphene nanoribbons<sup>29</sup>. Previous calculations<sup>12</sup> and experiments<sup>30</sup> have shown that O<sub>2</sub> in the triplet state is physisorbed on the surface of single-walled carbon nanotubes (SWCNTs) and graphene, and the transport properties could not be significantly affected. On the other hand, the electronic properties of carbon-doped boron nitride nanotubes can be changed dramatically by the chemisorption of O<sub>2</sub> molecule<sup>31</sup>. This indicates that the dopants can improve the reactivity of materials, and the O<sub>2</sub> molecules can give rise to very different properties. Therefore, how O<sub>2</sub> molecule can affect the properties of doped graphene is necessary to be understood in the fields of both gas sensing and electronics.

In this paper we study from first principles the adsorption of molecular oxygen on B-, N-, Al-, Si-, P-, Cr- and Mn-doped graphene. In order to illuminate easily, these materials are abbreviated to be BG, NG, AG, SG, PG, CG and MG. BG and NG retain a planar form, while

other atoms protrude out of the graphene layer and induce a local curvature in graphene. Furthermore, O<sub>2</sub> molecule is physisorbed on BG and NG with relatively small adsorption energy and large distance of X-O (X represents the doping atom), comparing with chemisorption on the doped graphene with other dopants. In the end, the chemisorption induces dramatic change for the electronic structures of doped graphene, and injects magnetic moments into the system except O<sub>2</sub> on PG. Especially, the system of O<sub>2</sub> on CG is antiferromagnetic (AFM).

## II. COMPUTATIONAL METHODS

Spin-polarized density-functional theory (DFT) calculations are performed using the Perdew-Burke-Ernzerhof (PBE)<sup>32</sup> generalized gradient approximation (GGA) for the exchange-correlation potential. A supercell of  $6 \times 6$  graphene including 72 C atoms with a doped atom substituting a C atom and a single O<sub>2</sub> molecule adsorbed onto it is constructed. With this model, the dopant concentration in our calculations is  $\sim 1.4\%$ . Experiments have shown the existence of these types of single-atom doped materials<sup>33</sup>. Besides, a method to synthesize the transition metals doped graphene has been proposed<sup>21</sup>. In the direction normal to the surface, 29.5 Å length in the supercell is sufficient to minimize the interaction between graphene layers. Ultrasoft pseudopotentials<sup>34</sup> and a plane-wave basis set-up to a kinetic energy cutoff of 25 Ry for the wave function and of 200 Ry for the charge density are chosen in all simulations (for transition metals Cr and Mn, a cutoff of 35 Ry for the wave function and 300 Ry for the charge density). The Brillouin zone is sampled using a  $3 \times 3 \times 1$  Monkhorst-Pack<sup>35</sup> grid and Methfessel-Paxton<sup>36</sup> smearing of 0.01 Ry. A denser  $11 \times 11 \times 1$  Monkhorst-Pack grid and the tetrahedron method<sup>37</sup> are used for the calculation of density of states (DOS) and partial DOS (PDOS). Atomic positions are optimized until the maximum force on any atom is less than 0.001 a.u. All calculations are performed using the Quantum-ESPRESSO package<sup>38</sup>. We carefully test this supercell for the convergence of energy, magnetic properties, comparing a larger supercell as in Ref. 21, and there is few difference found.

Here, we would like to point out that the usage of GGA, the consequent neglect of van der Waals interactions, leads to an incorrect description of physisorption, but this is of little concern for us since we are interested in chemically bound molecules. In fact, in physisorbed systems, LDA results look “better” than GGA, but they are just “wrong in a different way”. For chemically bound systems, GGA is usually a better choice.

In this calculation, only the triplet O<sub>2</sub> molecule is considered, which is the ground state of O<sub>2</sub>. The adsorption energy is defined by  $E_a = E_{tot} - E_{dg} - E_o$ , where  $E_{tot}$  is the total energy of the doped graphene with a bound O<sub>2</sub> molecule,  $E_{dg}$  is the energy of doped graphene and  $E_o$  is the energy of isolated O<sub>2</sub> molecule. In order to minimize

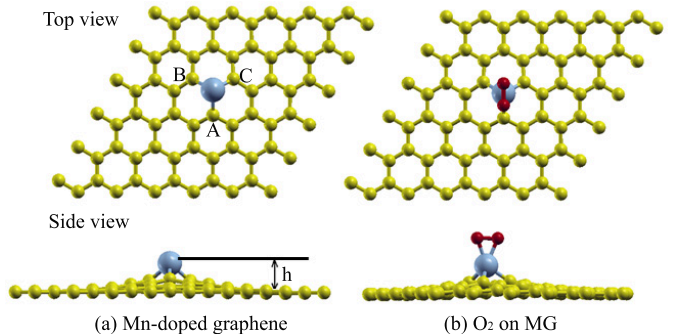


FIG. 1: (Color online) The most stable configurations of MG with an elevation  $h$  of 1.555 Å (a); and of O<sub>2</sub> on MG with  $h$  of 1.652 Å (b). Yellow: Carbon, Cambridge blue: Mn, Red: O, respectively.

systematic errors, the same supercells and  $k$ -point grids are used for all calculations.

## III. RESULTS AND DISCUSSION

The bond length of O<sub>2</sub> molecule in ground state is 1.2350 Å (experimental value is 1.207 Å) and the magnetic moment is  $2 \mu_B$  in our calculations. O<sub>2</sub> molecule is placed at the top of the doping atoms, and slightly inclined to the graphene plane at the beginning. After relaxation, O<sub>2</sub> molecule is found to be physisorbed on the top of B and N atoms, while chemisorbed on the top of Al, Si, P, Cr and Mn atoms. After relaxation, O<sub>2</sub> is parallel to graphene plane, which is the most stable configuration according to the test of our calculations. The configurations of MG and O<sub>2</sub> adsorption on MG are shown in Fig.1, where the Mn atom protrudes out of the graphene plane. All configurations here are very similar to Fig. 1, except for BG and NG with all atoms in the same plane and physisorbed O<sub>2</sub>. In fact, a metastable configuration with all atoms in one plane can be obtained if the dopant is set to be in the same plane of graphene, but it is very easy to transform to the stable one. Meanwhile, the results of O<sub>2</sub> adsorption on all doped graphene are shown in Table.I, which will be discussed detailedly below.

### A. adsorption of oxygen on CG and MG

We first discuss the adsorption of O<sub>2</sub> on CG and MG. The atomic and magnetic structures of CG and MG have been discussed in Ref. 21. As shown in Fig. 1 and Table. I, the elevation of Cr and Mn atoms is 1.6487 and 1.5555 Å; the Cr-C and Mn-C bond lengths are 1.8559 and 1.8317 Å; the magnetic moments are  $2.00\mu_B$  and  $3.00\mu_B$ , respectively. These are in good agreement with

TABLE I: Summary of atomic structures of the compounds, including adsorption energy  $E_a$  (eV), the shortest bond length of X-C  $d_{X-C}$ (Å), shorter bond length of X-O  $d_{X-O}$ (Å), bond length of O-O  $d_{O-O}$ (Å), the elevation of the dopant atoms above the graphene plane  $h$  (Å) (negative value means the dopants protrude out of the plane in opposite direction to O<sub>2</sub> molecule), magnetic moments of the system  $M_B$  ( $\mu_B$ ), and Löwdin charge<sup>39</sup> transfers from doped graphene to O<sub>2</sub> molecule  $c$  ( $e^-$ ).

		Cr	Mn	Al	Si	P	B	N
doped graphene	$h$	1.6487	1.5555	1.7584	1.4579	1.4591	0.0000	0.0000
	$d_{X-C}$	1.8559	1.8317	1.8528	1.7611	1.7689	1.4794	1.4079
	$M_B$	2.0000	3.0000	0.0000	0.0000	1.0500	0.0000	0.0000
O <sub>2</sub> adsorption	$E_a$	-2.6098	-2.0918	-1.5589	-1.3132	-1.0359	-0.0232	-0.1228
	$h$	1.6188	1.6520	1.9026	1.6607	1.4840	-0.2457	-0.0541
	$d_{X-C}$	1.8159	1.8464	1.9284	1.8284	1.7501	1.4810	1.4066
	$d_{X-O}$	1.7935	1.8641	1.8770	1.7109	1.6275	3.5099	3.3196
	$d_{O-O}$	1.4088	1.3993	1.4000	1.5103	1.5584	1.2354	1.2577
	$M_B$	AFM	1.4500	1.0000	0.3300	0.0000	1.9900	1.8000
	$c$	0.2166	0.1865	0.4367	0.9184	0.8181	-0.0863	0.0235

the results using a larger supercell in Ref. 21. The unpaired electrons in transition metals (Cr and Mn) induce magnetic moments, and the direction of spin polarization of Cr or Mn is opposite to that of the nearest carbon atoms, that is,  $C_A$ ,  $C_B$  and  $C_C$  in Fig. 1a.

From Table. I, we can learn the configurations are changed dramatically after O<sub>2</sub> adsorption. The molecular oxygen is chemisorbed on CG and MG with large adsorption energies of -2.6098 and -2.0918 eV, respectively, indicating very stable adsorption of O<sub>2</sub>. The bonds of Cr-O and Mn-O are formed with short lengths of 1.7935 and 1.8641 Å; The elevation of Cr above graphene plane is shortened to 1.6188 Å, while the elevation of Mn is extended to 1.6520 Å. The O-O bond extends to 1.4088 and 1.3993 Å for CG and MG. Interestingly, CG become AFM by the adsorption of O<sub>2</sub>, i.e., with zero total magnetic moment but 0.34 $\mu_B$  absolute magnetic moment. We calculate the magnetic moment of every atom in the system, and find the magnetic moment of Cr atom (-0.1435) is opposite to other atoms such as O (0.0411 $\mu_B$ , 0.0421 $\mu_B$ ), the three nearest C atoms  $C_A$  (0.0133 $\mu_B$ ),  $C_B$  (0.0169 $\mu_B$ ) and  $C_C$  (0.0169 $\mu_B$ ). At the same time, the absolute magnetic moment of Cr and the sum of magnetic moment of O,  $C_A$ ,  $C_B$  and  $C_C$  is very close. These two properties make the system AFM, and the magnetization very localized, as shown in Fig. 2a. For MG, O<sub>2</sub> adsorption reduces the magnetic moment of the system to 1.45  $\mu_B$ , which is caused by the decrease of unpaired electrons due to the hybridization between Mn and O atoms. Similar to O<sub>2</sub> on CG, the magnetic moment is located around the Mn atom, as shown in Fig. 2b, which may be a Kondo system.

In order to understand the electronic properties of the system, DOS and PDOS of O<sub>2</sub>-CG and O<sub>2</sub>-MG are calculated, as shown in Fig. 3 and 4, respectively. It is well known that intrinsic graphene is semimetal. In Fig. 3, it is obvious that CG is a metal. After adsorption of O<sub>2</sub>, the O, C and Cr hybridize strongly. There is one DOS peak for spin down electrons appearing at the Fermi level, which comes from the hybridization of Cr atom and O<sub>2</sub> molecule. One peak disappears below the position of -1.5

eV, which mainly belongs to the contribution of 3d electrons in Cr atom. Löwdin charge analysis shows there is 0.2166  $e^-$  transfer from CG to O<sub>2</sub> molecule, that is to say, O<sub>2</sub> is an acceptor here. Therefore, O<sub>2</sub> can actually p-dope the host CG, which is consistent with the effect of O<sub>2</sub> on organic semiconductors<sup>28</sup>. Similarly, O<sub>2</sub> can p-dope MG through accepting 0.1865  $e^-$ . From Fig. 4, we can learn that the change of electronic properties of MG induced by O<sub>2</sub> adsorption is mainly around the Fermi level, where the DOS peak of spin-down electrons of MG before adsorption above the Fermi level disappears, which is contributed by the 3d electrons in Mn atom hybridizing with 2p electrons in O atom. Meantime, one peak for spin-up electrons appears at the Fermi level, which is made up of hybridized Mn d and O p orbitals according to the PDOS analysis in Fig. 4. Similar to the analysis of spin density (Fig. 2), the magnetization is also localized and then O<sub>2</sub> adsorbed on Cr or Mn may exhibit as Kondo impurities as well as Cr or Mn doped into graphene<sup>21</sup> and Ni impurity in a Au nanowire<sup>40</sup>.

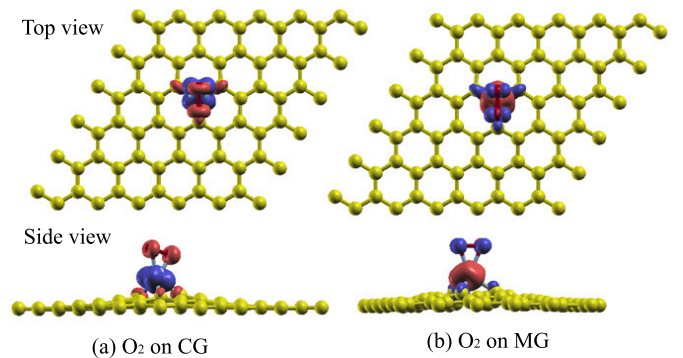


FIG. 2: (Color online) Spin density in O<sub>2</sub> adsorption on doped graphene. (a) O<sub>2</sub>-CG chemisorption system with isovalues of  $\pm 0.01$  a.u.; (b) O<sub>2</sub>-MG chemisorption system with isovalues of  $\pm 0.001$  a.u.. Blue color represents spin-down states, red color spin-up states.

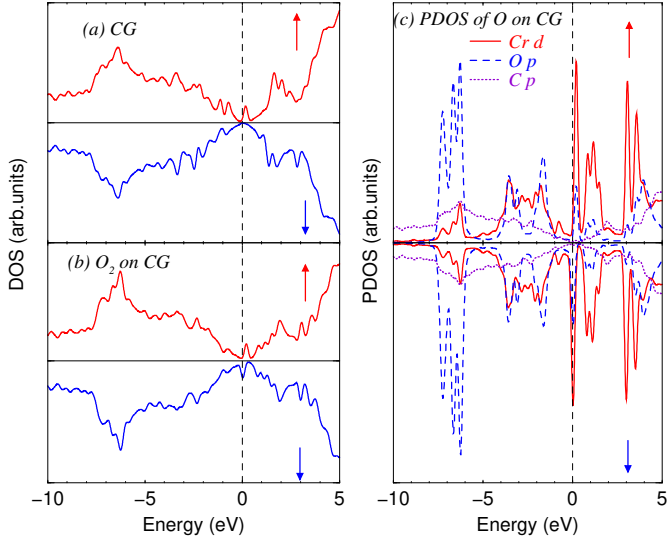


FIG. 3: (Color online) Total and partial DOS for CG and  $O_2$ -CG chemisorption system. (a) Total DOS of CG before adsorption of  $O_2$ ; (b) Total DOS of CG after adsorption of  $O_2$ ; (c) PDOS of atoms in  $O_2$ -CG chemisorbed system. PDOS of  $O_p$  is the average of two O atoms, and  $C_p$  is the average of all C atoms in the system. The arrows denote the spin-down ( $\downarrow$ ) states and spin-up ( $\uparrow$ ) states. The zero energy is the Fermi level.

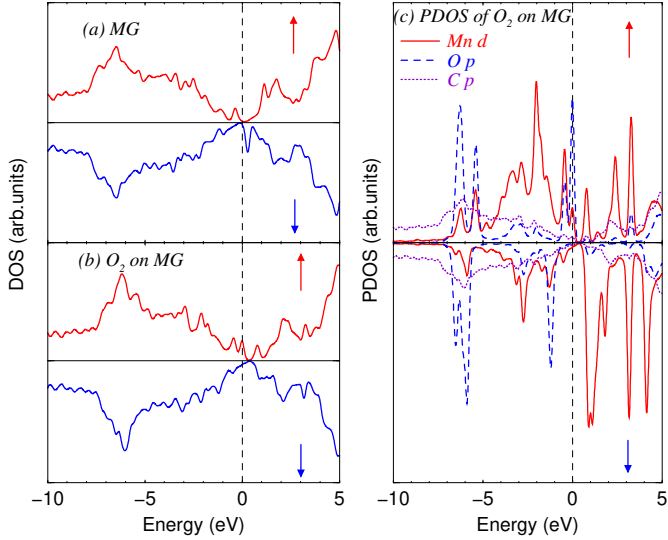


FIG. 4: (Color online) Total and partial DOS for MG and  $O_2$ -MG chemisorption system. (a) Total DOS of MG before adsorption of  $O_2$ ; (b) Total DOS of MG after adsorption of  $O_2$ ; (c) PDOS of atoms in  $O_2$ -MG chemisorbed system. The arrows denote the spin-down ( $\downarrow$ ) states and spin-up ( $\uparrow$ ) states. The zero energy is the Fermi level.

## B. adsorption of oxygen on AG, SG and PG

Al, Si and P elements contain  $3p$  orbital, and they have 3, 4 and 5 valence electrons respectively. Discussion about their doping into graphene and nanotubes has been reported recently, which show that they are potential resources for detecting toxic molecules and modulating the electronic structures of graphene.

From Table. I, we can learn that Al, Si and P atoms introduce a local curvature of graphene, with elevation of 1.7584, 1.4579 and 1.4591 Å, respectively. Meanwhile, the bond lengths of Al-C, Si-C and P-C is 1.8528, 1.7611 and 1.7689 Å, respectively, which basically decrease with the increase of electrons of the elements. In fact, for atoms which have the same configurations of orbitals, the covalent bond length decreases with the increase of group number. This indicates that the extension of electron states plays a very important role in the structures of doped graphene. Specially, P dopant introduces spin-polarization into the PG with magnetic moment of  $1.05 \mu_B$ , while no magnetization exists for AG and SG. It is noticed that a metastable configuration of PG with all atoms retaining in one plane can be observed, in which there is no spin polarization induced. It seems that the local curvature has a very important effect for the magnetic property.  $O_2$  molecule can be chemisorbed on the atoms of Al, Si and P in graphene, with large adsorption energies of -1.5589, -1.3132 and -1.0359 eV, respectively. Meantime, the atomic structures change much. For AG, Al atom has an elevation of 1.9026 Å, and C-Al bond extends to 1.9284 Å, Al-O to 1.8770 Å and O-O to 1.40 Å. For SG, Si atom protrudes out of graphene plane with elevation of 1.6607 Å. C-Si, Si-O and O-O bonds also elongate, which are 1.8284, 1.7109 and 1.5103 Å, respectively. On the contrary, chemisorption of  $O_2$  on PG shorten the P-C bond to 1.6286 Å from 1.7691 Å before adsorption, and the bond O-O is broken completely with the long distance of 1.5598 Å. The P atom almost retains the place above graphene with 1.4796 Å and does not protrude outward more. It is interesting that chemisorption of  $O_2$  introduces spin polarization for AG and SG with magnetic moments of  $1.00$  and  $0.33 \mu_B$ , but the magnetization in PG vanishes after  $O_2$  adsorption. For AG and SG, the spin-polarization is mainly located in the O atoms, which is also very localized as shown in Fig. 5. Therefore,  $O_2$  adsorption may introduce Kondo effect into AG and SG systems.

The electronic properties are also investigated by the analysis of DOS (PDOS) and Löwdin charges. For AG after adsorption, the analysis of Löwdin charges shows that  $O_2$  molecule accepts about  $0.44 e^-$  from Al atom, and  $0.72 e^-$  transfers from Al to the three nearest C atoms (0.24 per atom). The DOS of AG before and after adsorption of  $O_2$  is shown in Fig. 6. Al has 3 valence electrons, and therefore can be hole-doping for graphene, as shown in Fig. 6a, where the minimum of DOS shifts above the Fermi level. Chemisorption of  $O_2$  introduces spin polarization, which creates the difference of the DOS

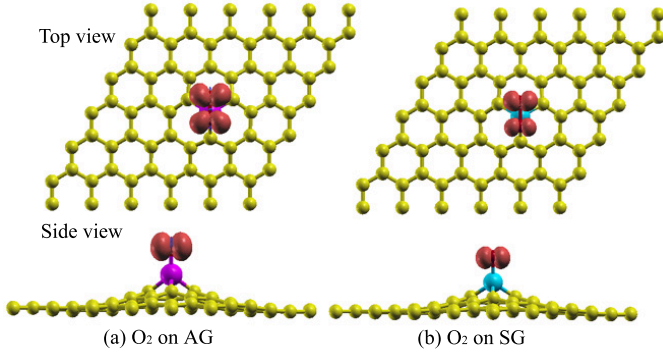


FIG. 5: (Color online) Spin density in  $O_2$  adsorption on doped graphene. (a) in  $O_2$ -AG chemisorption system; (b)  $O_2$ -SG chemisorption system. Blue color represents spin-down states, red color spin-up states. The isovalues are  $\pm 0.002$  a.u.

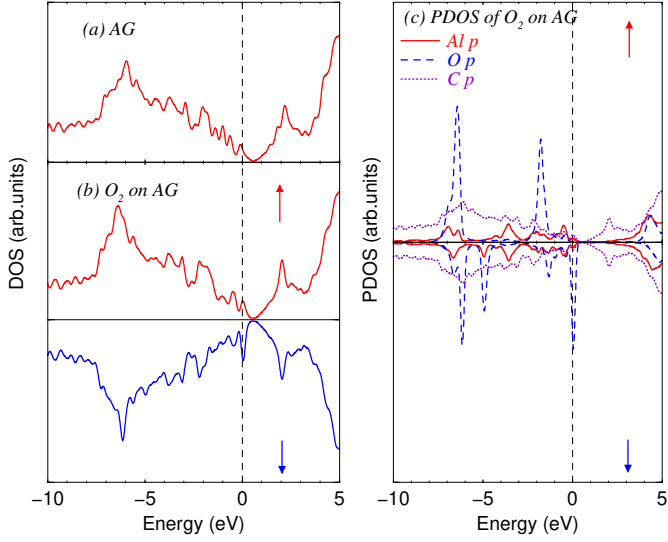


FIG. 6: (Color online) Total and partial DOS for AG and  $O_2$ -AG chemisorption system. (a) Total DOS of AG before adsorption of  $O_2$ ; (b) Total DOS of AG after adsorption of  $O_2$ ; (c) PDOS of atoms in chemisorbed system. The arrows denote the spin-down ( $\downarrow$ ) states and spin-up ( $\uparrow$ ) states. The zero energy is the Fermi level.

mainly around the Fermi level, as shown in Fig. 6b. The peak at Fermi level for spin down electrons is contributed by the  $O_p$  orbital according to the PDOS analysis, shown in Fig. 6c.

For chemisorption of  $O_2$  on SG,  $O_2$  molecule accepts about  $0.92 e^-$  from Si atom, and about  $0.23 e^-$  transfers from Si atom to every nearest C atom. Si has 4 electrons, the same as C atom. Therefore, the doping of Si should not shift the Fermi level of graphene, as shown in Fig. 7a. It is worth pointing out that the electronic structures are dependent on the dopant concentration, as shown in Fig. 7b, and the electronic band of SG system is open with a gap of 0.1 eV. Nevertheless, it does not affect the configuration of chemisorption of  $O_2$  on SG.  $O_2$

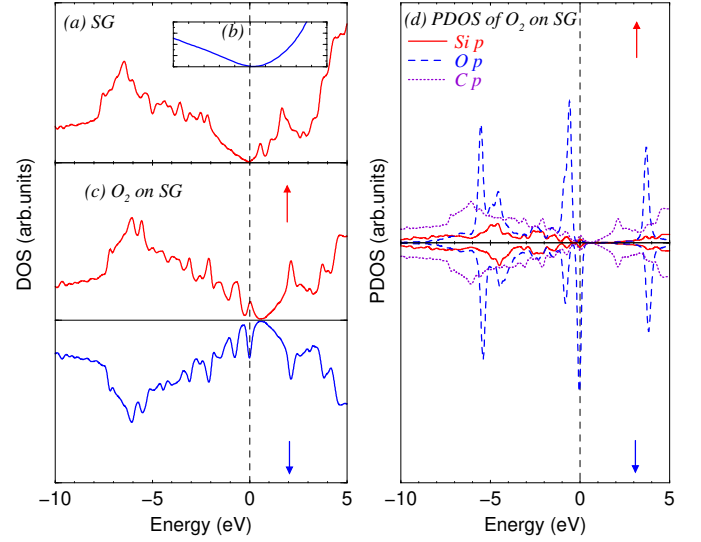


FIG. 7: (Color online) Total and partial DOS for SG and  $O_2$ -SG chemisorption system. (a) Total DOS of SG before adsorption of  $O_2$ ; (b) DOS of SG with 3% concentration; (c) Total DOS of SG after adsorption of  $O_2$ ; (d) PDOS of atoms in chemisorbed system. The arrows denote the spin-down ( $\downarrow$ ) states and spin-up ( $\uparrow$ ) states. The zero energy is the Fermi level.

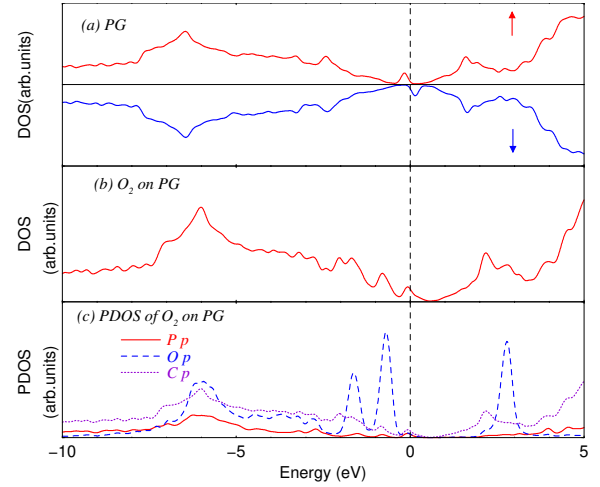


FIG. 8: (Color online) Total and partial DOS for PG and  $O_2$ -PG chemisorption system. (a) Total DOS of PG before adsorption of  $O_2$ ; (b) Total DOS of PG after adsorption of  $O_2$ ; (c) PDOS of atoms in chemisorbed system. The arrows denote the spin-down ( $\downarrow$ ) states and spin-up ( $\uparrow$ ) states. The zero energy is the Fermi level.

adsorption introduces magnetization with  $0.33 \mu_B$ . As shown in Fig. 7c-d, the difference of the DOS between spin up and spin down electrons is mainly caused by  $O_p$  orbital. The DOS peak of spin up electrons at the Fermi level is caused by the  $p_z$  orbital in C atom, while the peak of spin down by  $O_p$ . Moreover, the hybridization of  $Si_p$ ,  $O_p$  and  $C_p$  orbitals also happens here.

For  $O_2$  on PG, about  $0.82 e^-$  transfers from P atom to two O atoms, and about  $0.24 e^-$  from P atom to every nearest C atom. Before  $O_2$  binding, PG is magnetic with  $1.05 \mu_B$ . Here, charge analysis shows us that every nearest C atom accepts about  $0.18 e^-$  from P atoms, and about  $4.3 e^-$  remains in P atoms. That is to say, there is about one electron unpaired, inducing about  $1 \mu_B$  magnetic moment. After adsorption of  $O_2$ , the hybridization between P and O, even including C, employs the unpaired electron, and then the spin polarization vanishes. According to the DOS of PG before adsorption of  $O_2$ , as shown in Fig. 8a, the difference of DOS between spin up and spin down electrons mainly locates around the Fermi level. The binding of  $O_2$  evaporates the magnetization and creates a peak at the position of  $-0.75 eV$ , as shown in Fig. 8b, which is caused by the hybridization of  $Pp$ ,  $Op$  and  $Cp$  orbitals, as shown in Fig. 8c.

### C. Adsorption of oxygen on BG and NG

B and N belong to the second group elements in the periodic table, which have  $2s2p$  configurations for electrons and are the nearest elements for C. The extension of electrons of B, C and N is similar. Therefore, there is no local distortion when B and N are doped in graphene. The length of B-C is  $1.4794 \text{ \AA}$ , larger than that of N-C with  $1.4079 \text{ \AA}$ . B and N atoms do not have elevation above graphene, and there is also no spin polarization.  $O_2$  is physisorbed on BG and NG, which is the same as  $O_2$  on B-doped graphite<sup>41</sup>. The physisorption does not change the structures of BG and NG significantly, and the magnetic moments of  $O_2$  is also almost retained, as shown in Fig. 9a. The spin density of  $O_2$ -NG is very similar. The spin density of  $O_2$ -BG system concentrates in the  $O_2$  molecule, which is almost the same as the spin density of isolated  $O_2$  molecule, shown in Fig. 9b. The  $O_2$  molecule is far away from graphene with a distance larger than  $3.5 \text{ \AA}$  and a relatively small adsorption energy. Furthermore, B and N atoms is slightly pushed below graphene plane by  $O_2$ , indicating the repulsed force between them. Since B and Al, N and P belong to the same group elements and have very similar valence electron configurations, and their behaviors caused by  $O_2$  molecule are so different, it can be induced that one important reason for this phenomenon is the local curvature in AG and PG. This is also in agreement with the conclusion of local curvature enhancing chemical reactivity of doped graphene<sup>19</sup>. About this local curvature, as in Table. I, only the B and N dopants are not elevated, and the B-C and N-C bond lengths are close to C-C bond in graphene. By contrary, other dopants are elevated, and the X-C bonds are much longer than C-C bonds. Therefore, it can be concluded that dopant X is elevated only when the length of X-C is appreciably larger than that of C-C.

Although  $O_2$  can not bind stably on BG and NG, it can still affect the electronic properties at low temperature at

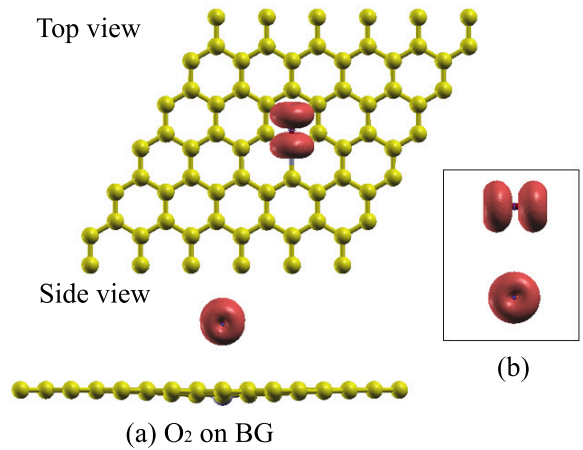


FIG. 9: (Color online) Spin density in  $O_2$  adsorption in (a)  $O_2$ -BG physisorption system, and (b) isolated  $O_2$ . The iso-values are  $\pm 0.005$  a.u.

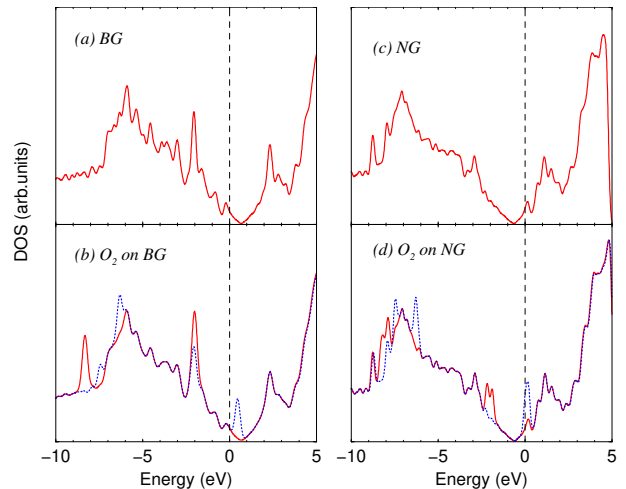


FIG. 10: (Color online) (a) Total DOS of BG before adsorption of  $O_2$ ; (b) Total DOS of BG after adsorption of  $O_2$ ; (c) Total DOS of NG before adsorption of  $O_2$ ; (d) Total DOS of NG after adsorption of  $O_2$ ; Red solid line represents spin-up states and blue dashed line spin-down states in (b) and (d). The zero energy is the Fermi level.

least. The dopant of Boron can hole-dope graphene and Nitrogen electron-dope graphene, as shown in Fig. 10a,c, where the Dirac point shifts above (BG) or below (NG) the Fermi level. After adsorption of  $O_2$ , the spin polarization is introduced and the DOS is changed. One DOS peak around Fermi level appears for spin down electrons of BG and NG physisorbed  $O_2$  molecule, caused by  $Op$  orbital; but the DOS of spin up electrons is very similar to that of BG before adsorption. This means that the change in DOS is concentrated on the  $O_2$  molecule. However, this effect should not exist at room temperature because of the very weak adsorption and the long distance between  $O_2$  and graphene. Furthermore, the

charge transfer between O<sub>2</sub> and BG or NG is very small compared with the chemisorption, indicating the small change for the conductance of the system. It should be noticed that O<sub>2</sub> acts as a donor for BG through donating  $\sim 0.08 e^-$  to BG system. Although the charge transfer of the physisorbed system using the figure of the single electron Kohn-Sham equation is under debate, the trend of this small charge transfer is reliable.

#### IV. CONCLUSION

In conclusion, our simulation studies reveal that most of doped graphene are sensitive to O<sub>2</sub> molecule. The local curvature caused by doped atoms is very important to the reactivity for gas molecules. BG and NG are inert to molecular oxygen, while graphene with Al, Si, P, Cr and Mn doping allows O<sub>2</sub> to form stable chemisorption states, which affects the magnetic, electronic and atomic properties of graphene. O<sub>2</sub> acts as an acceptor in all chemisorbed configurations, and introduces localized spin polarization except on PG. In particular, O<sub>2</sub> on CG is AFM, and O<sub>2</sub> can retain its magnetic moments on B- and N-doped graphene. Significantly, O<sub>2</sub> adsorption

may introduce Kondo effect into CG, MG, AG and SG systems. Most of systems with O<sub>2</sub> on doped graphene behave as metallic materials. Therefore, a combination of foreign atom doping followed by exposure to air may be an effective way to tune the electronic and magnetic properties of semimetal and unpolarized graphene. However, the potential usage of doped graphene as gas sensors should be dependent on the sensitivity to O<sub>2</sub> molecule in air. When chemisorption of O<sub>2</sub> on doped graphene happens, the sensitivity to other gases should be affected significantly, which may prevent it from being effective gas sensors.

#### V. ACKNOWLEDGMENTS

This work is supported by the National Natural Science Foundation of China under Grant Nos. 10734140 and 60621003, the National Basic Research Program of China (973 Program) under Grant No. 2007CB815105, and the National High-Tech ICF Committee in China. All calculations are carried at the Research Center of Supercomputing Application, NUDT.

- 
- \* Electronic address: [jmyuan@nudt.edu.cn](mailto:jmyuan@nudt.edu.cn)
- <sup>1</sup> K. S. Novoselov, A. K. Geim, S. V. Morozov, D. Jiang, Y. Zhang, S. V. Dubonos, I. V. Grigorieva, and A. A. Firsov, *Science* **306**, 666 (2004).
  - <sup>2</sup> A. K. Geim and K. S. Novoselov, *Nat. Mater.* **6**, 183 (2007).
  - <sup>3</sup> A. H. Castro Neto, F. Guinea, N. M. R. Peres, K. S. Novoselov and A. K. Geim, *Rev. Mod. Phys.* **81**, 109 (2009).
  - <sup>4</sup> F. Schedin, A. K. Geim, S. V. Morozov, E. W. Hill, P. Blake, M. I. Katsnelson and K. S. Novoselov, *Nat. Mater.* **6**, 652 (2007).
  - <sup>5</sup> K. S. Novoselov, A. K. Geim, S. V. Morozov, D. Jiang, M. I. Katsnelson, I. V. Grigorieva, S. V. Dubonos and A. A. Firsov, *Nature* **438**, 197 (2005).
  - <sup>6</sup> Y. Zhang, J. Tan, H. L. Stormer and P. Kim, *Nature* **438**, 201 (2005).
  - <sup>7</sup> R. Danneau, F. Wu, M. F. Craciun, S. Russo, M. Y. Tomi, J. Salmilehto, A. F. Morpurgo and P. J. Hakonen, *Phys. Rev. Lett.* **100**, 196802 (2008).
  - <sup>8</sup> T. Ohta, A. Bostwick, T. Seyller, K. Horn and E. Rotenberg, *Science* **313**, 951 (2006).
  - <sup>9</sup> T. G. Pedersen, C. Flindt, J. Pedersen, N. A. Mortensen, A. P. Jauho, and K. Pedersen, *Phys. Rev. Lett.* **100**, 136804 (2008); B. Trauzettel, D. V. Bulaev, D. Loss, and G. Burkard, *Nat. Phys.* **3**, 192 (2007); A. Rycerz, J. Tworzyd, and C. W. J. Beenakker, *Nat. Phys.* **3**, 172 (2007).
  - <sup>10</sup> B. Huang, Z. Li, Z. Liu, G. Zhou, S. Hao, J. Wu, B.-L. Gu, and W. Duan, *J. Phys. Chem. C* **112**, 13442 (2008); R. Moradian, Y. Mohammadi, and N. Ghobadi, *J. Phys. Cond. Matt.* **20**, 425211 (2008).
  - <sup>11</sup> O. Leenaerts, B. Partoens and F. M. Peeters, *Phys. Rev. B* **77**, 125416 (2008).
  - <sup>12</sup> P. Giannozzi, R. Car and G. Scoles, *J. Chem. Phys.* **118**, 1003 (2003).
  - <sup>13</sup> J. Dai, P. Giannozzi and J. Yuan, *Surf. Sci.* **603**, 3234 (2009).
  - <sup>14</sup> Y. Zhang, Y. Chen, K. Zhou, C. Liu, J. Zeng, H. Zhang and Y. Peng, *Nanotechnology* **20**, 185504 (2009).
  - <sup>15</sup> J. Dai, J. Yuan and P. Giannozzi, *Appl. Phys. Lett.* **95**, 232105 (2009).
  - <sup>16</sup> E. Rangel, G. R. Chavarria and L. F. Magana, *Carbon* **47**, 531 (2009).
  - <sup>17</sup> H. Jiang, D. Zhang and R. Wang, *Nanotechnology* **20**, 145501 (2009).
  - <sup>18</sup> S. Dutta and S. K. Pati, *J. Phys. Chem. B*, **112**, 1333 (2008).
  - <sup>19</sup> A. L. E. Garcia, S. E. Baltazar, A. H. Romero, J. F. Perez Robles and A. Rubio, *J. Comput. Theor. Nanosci.* **5**, 2221 (2008).
  - <sup>20</sup> N. Gorjizadeh, A. A. Farajian, K. Esfarjani and Y. Kawazoe, *Phys. Rev. B* **78**, 155427 (2008); E. J. G. Santos, A. Ayuela, S. B. Fagan, J. Mendes Filho, D. L. Azevedo, A. G. Souza Filho and D. Sánchez-Portal, *Phys. Rev. B* **78**, 195420 (2008).
  - <sup>21</sup> A. V. Krasheninnikov, P. O. Lehtinen, A. S. Foster, P. Pyykko and R. M. Nieminen, *Phys. Rev. Lett.* **102**, 126807 (2009).
  - <sup>22</sup> Y. Mao and J. Zhong, *Nanotechnology* **19**, 205708 (2008).
  - <sup>23</sup> S. Lakshmi, S. Roche, and G. Cuniberti, *Phys. Rev. B* **80**, 193404 (2009).
  - <sup>24</sup> A. Nduwimana and X. Q. Wang, *ACS Nano* **3**, 1995 (2009); G. Cantele, Y. S. Lee, D. Ninno, and N. Marzari, *Nano Lett.* **9**, 3425 (2009); Y. H. Zhang, K. G. Zhou, K. F. Xie, J. Zeng, H. L. Zhang, and Y. Peng, *Nanotechnology* **21**, 065201 (2010).

- <sup>25</sup> D. Wei, Y. Liu, Y. Wang, H. Zhang, L. Huang and G. Yu, *Nano. Lett.* **9**, 1752 (2009).
- <sup>26</sup> L. S. Panchakarla, K. S. Subrahmanyam, S. K. Saha, A. Govindaraj, H. R. Krishnamurthy, U. V. Waghmare and C. N. R. Rao, *Adv. Mater.* **21**, 4726 (2009).
- <sup>27</sup> I. O. Maciel, J. Campos-Delgado, E. Cruz-Silva, M. A. Pimenta, B. G. Sumpter and V. Meunier, F. López-Urías, E. Muñoz-Sandoval, H. Terrones, M. Terrones and A. Jorio, *Nano. Lett.* **9**, 2267 (2009).
- <sup>28</sup> C. Lu and H. Meng, *Phys. Rev. B* **75**, 235206 (2007).
- <sup>29</sup> J. Berashevich and T. Chakraborty, *Phys. Rev. B* **80**, 033404 (2009); T.O. Wehling et al, *Nano Lett.* **8**, 173 (2008); S.S. Yu et al, *IEEE TRANSACTIONS ON NANOTECHNOLOGY* **7**, 628 (2008).
- <sup>30</sup> H. Ulbricht, G. Moos and T. Hertel, *Surf. Sci.* **532**, 852 (2003).
- <sup>31</sup> J. Zhang, K. P. Loh, J. Zheng, M. B. Sullivan and P. Wu, *Phys. Rev. B* **75**, 245301 (2007).
- <sup>32</sup> J. P. Perdew, K. Burke and M. Ernzerhof, *Phys. Rev. Lett.* **77**, 3865 (1996).
- <sup>33</sup> P. M. Voyles, D. A. Muller, J. L. Grazul, P. H. Citrin, and H. J. L. Gossmann, *Nature* **416**, 826 (2002); C. I. Pakes, D. P. George, D. N. Jamieson, C. J. Yang, A. S. Dzurak, E. Gauja and R. G. Clark, *Nanotechnology* **14**, 157 (2003).
- <sup>34</sup> The pseudopotentials of B.pbe-n-van.UPF, C.pbe-van\_bm.UPF, O.pbe-van\_bm.UPF, N.pbe-van\_bm.UPF, Al.pbe-n-van.UPF, Si.pbe-n-van.UPF, P.pbe-n-van.UPF, Cr.pbe-sp-van.UPF and Mn.pbe-sp-van.UPF from the Quantum ESPRESSO distribution.
- <sup>35</sup> H. J. Monkhorst and J. D. Pack, *Phys. Rev. B* **13**, 5188 (1976).
- <sup>36</sup> M. Methfessel and A. T. Paxton, *Phys. Rev. B* **40**, 3616 (1989).
- <sup>37</sup> P. E. Blöchl, O. Jepsen and O. K. Andersen, *Phys. Rev. B* **49**, 16223 (1994).
- <sup>38</sup> P. Giannozzi *et al*, *J. Phys.: Condens. Matter* **21** 395502 (2009). URL: [www.quantum-espresso.org](http://www.quantum-espresso.org).
- <sup>39</sup> P. O. Löwdin, *J. Chem. Phys.* **18**, 365 (1950).
- <sup>40</sup> P. Lucignano, R. Mazzarello, A. Smogunov, M. Fabrizio and E. Tosatti, *Nat. Mater.* **8**, 563 (2009); K. Sengupta and G. Baskaran, *Phys. Rev. B* **77**, 045417 (2008).
- <sup>41</sup> Y. Ferro, A. Allouche, F. Marinelli and C. Brosset, *Surf. Sci.* **559**, 158 (2004).